

Impact of High Velocity Cold Spray Particles

R. C. Dykhuizen, M. F. Smith, D. L. Gilmore, and R. A. Neiser
Sandia National Laboratories*
Albuquerque, NM 87185-0835

X. Jiang and S. Sampath
Center for Thermal Spray Research
Department of Materials Science and Engineering
State University of New York at Stony Brook*
Stony Brook, NY11794-2275

*Sandia is a multiprogram laboratory operated by Sandia Corporation, a Lockheed Martin Company, for the United States Department of Energy under Contract DE-AC04-94AL85000. The work at SUNY was supported in part by the MRSEC program of National Science Foundation under award 96-32570.

Key Words: Cold Spray, Coating, Experimental, Analytic

Abstract

This paper presents experimental data and an analytical model of the cold spray solid particle impact process. Copper particles impacting onto a polished stainless steel substrate are examined. The high velocity impact causes significant plastic deformation of both the particle and the substrate, but no melting is observed. The plastic deformation exposes clean surfaces that, under the high impact pressures, result in significant bond strengths between the particle and substrate. Experimental measurements of the splat and crater sizes compare well with the numerical calculations. It is shown that the crater depth is significant and increases with impact velocity. However, the splat diameter is much less sensitive to the impact velocity. It is also shown that the geometric lengths of the splat and crater scale linearly with the diameter of the impacting particle. It is hoped that the results presented will allow better understanding of the bonding process during cold spray.

1. Introduction

Cold Spray Processing (or simply cold spray) is a high-rate material deposition process in which

small, unmelted powder particles (typically 1 - 50 microns in diameter) are accelerated to velocities on the order of 500 m/s and greater by a supersonic gas jet. Upon impact with a target surface, the solid particles and the substrate deform greatly. Successive impacts result in a continuous coating of the substrate with good bond strength (McCune et al., 1995). Cold spray was developed in the mid-1980's at the Institute of Theoretical and Applied Mechanics of the Siberian Division of the Russian Academy of Science in Novosibirsk (Alkhimov, et al., 1994; Tokarev, 1996). A recent article examined analytically the acceleration of the particles by the supersonic nozzle (Dykhuzen and Smith, 1998). That article also described the cold spray processing equipment and summarizes the advantages of the cold spray process over other spray coating processes. Gilmore, et al., 1998, presented experimental data for velocity and deposition efficiency of cold spray particles, and compared data to an analytical model.

The actual mechanisms by which the solid state particles deform and bond has not been well characterized. It seems plausible, though it has not yet been demonstrated, that plastic deformation may disrupt thin surface films, such as oxides, and provide intimate conformal contact under high local pressure, thus permitting bonding to occur. This hypothesis is consistent with the fact that a wide range of ductile materials, such as metals and polymers, have been cold spray deposited. Experiments with non-ductile materials, such as ceramics, have not been successful unless they are co-deposited along with a ductile matrix material. This theory would also explain the observed minimum critical velocity necessary to achieve deposition, since sufficient kinetic energy must be available to plastically deform the solid material enough to break up surface oxides.

This paper provides experimental measurements of the particle splats and impact craters. Also, numerical model simulations of the impact process are presented. The two methods show reasonable agreement. By combining experimental results and numerical modeling, the disadvantages of each are minimized. The experimental technique does not allow an exact description of each impact event. The impact velocity that corresponds to each individual crater is not available. However, a

particle velocity distribution is obtained from each experimental condition. The exact size, shape and orientation of the individual impacting particles are also unknown. However, the volume of the impacting particle is determined from the total volume of the resulting splat.

Use of a numerical model provides definition of the each impacting event, and allows variation of any parameter to obtain trends. However, the numerical model is limited by any inaccuracy that may exist in describing the high strain rate impact event.

2. Experimental Results

The Sandia cold spray facility was used to produce copper particle impacts onto a polished 304 stainless steel substrate. Details of the experimental setup are provided by Gilmore, et al., 1998. To enable examination of individual impacts, the operation was only modified to greatly decrease the powder flux. This was simply done by turning off the powder carrier gas just prior to the pass of the gun over the substrate. Due to the vertical orientation (spraying downward), and the relatively low powder velocity at injection during normal operation, it was thought that this change did not significantly alter the powder impact velocity during our experiments from the typical conditions of operation.

The cold spray system parameters were varied to yield mean particle impact velocities from 400 to 700 meters per second in increments of 100 meters per second. The actual mean velocities were 403, 521, 606 and 704 meters per second. From here on, the nominal mean velocities will be used. These conditions resulted in deposition efficiencies of copper onto stainless steel from 0% at the 400 m/s condition to 98% at the 700 m/s condition. These deposition efficiencies were found to be higher than measured for the same copper particles onto an aluminum substrate (Gilmore, 1998).

It should be noted that even though the results are presented as a function of the impact velocity, individual splats are created during a single experimental run from a variety of particle sizes. These particles each had velocities that were distributed about the mean. Typically, the smaller particles will travel faster (Neiser, et al., 1995). The standard deviation in the velocity was measured to be about 10% of the mean for all experimental conditions.

Figure 1 shows the gas atomized powder used in these experiments. As can be seen from the figure, the powder was reasonably spherical. The powder diameter was measured by a Coulter laser diffraction system and found to have a mean of 22 microns with a standard deviation of 5.6 microns. Metallography of particle cross-sections (not shown) indicated that the powder was near full density.

The deposited splats were examined by cross-sectioning the splat after deposition. A typical result is shown in Figure 2 for a 700 meter per second impact. Note the crater created in the stainless steel substrate. Also note that some of the ejected steel appears on the lower surface near the edge of the splat. This procedure proved unsuitable for obtaining accurate data since the process was not accurate enough to determine if the splat was cut through its center. This made determination of the particle size difficult.

Therefore, an alternate procedure was used to examine the splats produced. The deposited splats were examined using a scanning white light interferometer (De Groot, 1995) to determine the shape of the top surface. This provided quantitative information about the splat volumes. Due to the limitations of the system, overhangs resulted in a vertical profile, since the laser light can not examine underneath an overhang.

After the initial profilometry, the copper splats were dissolved by nitric acid. Careful weighing of

substrates before and after exposure to the acid revealed that substrate was not attacked by the etchant. By repositioning the profilometer above the previously examined locations, the craters that existed underneath each of the splats could then be measured. It is likely that the small thicknesses of stainless steel that form on the underside of overhangs (Figure 2) are not be preserved.

Figure 3 shows the output of the profilometer “before” and “after” the removal of a copper splat for an 600 meter per second impact. It is seen that a significant crater is formed in the stainless steel substrate. Also, note that the crater formed is not axi-symmetric. This may be due to the anisotropic nature of the impact that results from a projectile size that is smaller than the grain size of the stainless steel, which was found to be between 30 and 65 microns. Finally, the near vertical sides resolved by the profilometer may be indicative of the same overhang depicted in Figure 2.

From the profilometer measurements, estimates can be obtained for the volumes of various regions. The volume of material above a reference plane (the mean undeformed surface) was measured from the “before” image. Also from the “after image, the volume of material above and the volume of the crater below the reference surface was measured. Due to conservation of substrate volume, these two numbers correlated well. However, experimental measurement errors and difficulty in setting a reference surface level, resulted in some disagreement.

By a simple subtraction of the “before” and “after” heights, and integration over the splat surface, the volume of the impacting copper particle was determined. Or equivalently, the volume of the particle can be determined from a combination of the volumes determined above and below the reference surfaces. From the particle volume, an equivalent diameter of each copper particle was estimated (assuming fully dense spheres before impact).

It should be noted that the measured deposition efficiency for the 400 meter per second impact ve-

locity run was essentially zero. In fact, it was not possible to find 70 splats to measure (as was done for the other conditions). The 400 meter per second data set only consists of 26 splats. There were many empty craters found in the substrate for this condition, which indicated impacts without bonding. It is likely that the profilometer data for the 400 meter per second data is skewed towards the higher velocity particles in the distribution. And since the smaller than average particles will achieve a higher than average velocity, it is these particles that will bond to the substrate and be counted by our process. This is indeed observed. Figure 4 shows the equivalent diameter of the recovered splats as a function of the impacting velocity. It is seen that the mean particle diameter for the 400 m/s experiment is lower than those measured for the other experimental conditions.

As can be seen from Figure 4, the equivalent particle diameter is reasonably approximated by the 22 micron measurement of the original particle diameter for the faster data sets. In the data reduction process, there was significant effort to sample the entire range of splat sizes. With this criterion, it was difficult to maintain the proper proportion of each splat size so that the exact means could be reproduced. However, it was still intended that the mean of the each sampled subset would be representative of the process.

It was found that the crater depth is a strong function of the impact velocity. This is shown in Figure 5 where the crater volume presented is scaled by the volume of the copper particle that caused the crater. This plot shows that the crater volume increases significantly with the impact velocity. Again, the graph presents mean values for the data sets obtained at each velocity. The standard deviation for the non-dimensional crater volume is approximately 50% of the mean. This large amount of scatter is potentially due to experimental error in the profilometer measurements and integration of the profilometer data, various non-spherical geometries, variations in angle of impact, and variations in the actual impact velocity (scatter about the mean).

Figure 5 also shows the mean of the ratio of the splat diameter to the equivalent particle diameter

as a function of the mean impact velocity. This ratio is often called a flattening ratio. It is seen that the flattening ratio is relatively insensitive to the impact velocity (Again mean values are presented in the plot.). The standard deviation of the flattening ratio is only 10% of the mean.

The fact that the non-dimensional crater volume data used to generate Figure 5 has a 50% standard deviation versus only a 10% standard deviation for the flattening ratio data is due to the variations in the impact velocity within each experiment. Since the flattening ratio is insensitive to the impact velocity, variations of the impact velocity will not result in variations of the flattening ratio. However, the non-dimensional crater volume is sensitive to the impact velocity. Therefore, the known variations of the impact velocities result in variations in the crater volume.

The scatter in the experimental data is greatly reduced by our procedure of scaling the measurements with the volume (or diameter) of the individual impacting particle. This is shown in Figure 6 by a cross plot of the particle volume and the crater volume for the 500 m/s data set. The large amount of scatter in both quantities is shown. However, this plot also clearly shows the correlation between these two quantities. The ratio of the largest to smallest particle volume obtained from the data in Figure 6 is a factor of 43. This is equivalent to a factor of 3.5 in the particle diameter, which is equal to the ratio of smallest particle to largest particle diameter from our examination of the powder. This gives us confidence in the data collection process. Errors in determining the original particle diameter are due to profilometry measurement errors, interpolation of the profilometry during the integration process, and porosity of the powder which would disappear during the impact. Thus, perfect agreement between the particle sizes obtained from the two methods is not expected.

The non-dimensional crater volume is plotted against the particle size (for the 600 meter per second data set) in Figure 7. This reveals that that there is a tendency for smaller particles to have a greater

portion of their volume below the substrate surface. This is further indication that the smaller particles travel faster when exposed to the same gas conditions.

The bonding mechanism is of great interest. It has been proposed that large deformations and pressures are required in order to achieve intimate contact of clean metal surfaces. In this way, the bonding process is very similar to the explosive welding process (Crossland, 1982 and El-Sobky, 1983). It is generally accepted that the formation of a solid state “jet” of metal at the impact point of two metal plates promotes good bonding in explosive welding. Thus, the geometry and impact velocities are adjusted to assure that this jet forms at the moving contact point. This jet is credited with breaking up any surface layers and causing better contact of the two metal plates. Examination of the craters created in the cold spray process reveals evidence of jet formation. Figure 2 shows that both stainless steel and copper can be ejected from the crater. Figure 8 compares the craters created from an impact event where bonding has occurred and one where it did not. Both craters depicted in Figure 8 came from the same substrate, which was exposed to impacts that averaged near 500 meters per second. However, it is likely that the empty crater is the result from a slower than average impact. The measured deposition efficiency was 9% for this experimental condition and the standard deviation in the velocity was 60 meters per second. In general, crater lips appear sharper in the craters where the particle has bonded, while empty craters appear smoother. Due to the profilometry process, overhangs, as shown in Figure 2, are not seen. It is proposed that the sharper lip is an indication of large deformations that may result in exposure of clean fresh surfaces for bonding.

3. Numerical Results

A numerical model was set up to investigate the impact process. This model enabled examination

of trends in the impact process with various changes in the input that were not possible experimentally. For example, the experiments could only determine a probability density function for the impact velocity of each crater. So much of the experimental scatter was due to a distribution in the velocity of the particles that created the various craters at each system setting.

The Sandia generated computer code CTH (Hertel, 1993) was developed to model a wide range of solid dynamics problems involving shock wave propagation and material motion in one, two or three dimensions. The code uses a two-step Eulerian solution scheme. The first step is a Lagrangian step in which the cells distort to follow the material motion. The second step is a remesh step where the distorted cells are mapped back to the original Eulerian mesh. The mesh size used is 0.2 micron in both radial and axial directions. Larger mesh sizes resulted in predictions that were grid size dependent.

The simulations presented in this paper are normal angle impacts of fully dense spherical particles. This allowed the assumption of an axi-symmetric two-dimensional geometry. CTH includes various models for material properties. These material models predict the viscoplastic response of various materials (principally metals) based on a consideration of thermally-activated dislocation mechanics. The assumed forms take into account the effects of isotropic strain-hardening, thermal softening, strain rate dependency, and pressure-dependent shear and yield strengths. All of the available material models were investigated, each of which gave slightly different splat shapes. However, they all gave the same general trends as reported in this paper.

In the results presented in this paper, the Steinberg-Guinan-Lund (Steinberg, et al. 1980; Steinberg and Lund, 1989) viscoplastic model was used to model the stainless steel substrate. Rate dependent parameters were not available for this material. However, this model has been successfully used in other impact studies at Sandia for stainless steel targets. The Zerilli Armstrong model (Zerilli and Armstrong, 1987) was used for the copper particles. This model includes history and rate depen-

dent parameters to describe the mechanical response of the copper.

The substrate modeled is 200 microns in diameter. Figure 9 shows the final splat shape in cross-section that is obtained from a CTH run using a 25 micron particle impacting at various velocities onto a stainless steel substrate. Detailed examination of the numerical output reveals a peak temperature of 1200 K is obtained for the 700 meter per second impact (which is below the copper melting temperature of 1360 K). In fact, CTH overestimates material temperatures since dissipation via conduction is not modeled. When these calculations are rerun with a 20 micron particle, the geometric results are all scaled proportionally, which agrees with the experimental observations.

The 400 meter per second impact results in the lowest impact pressure and lowest deformations as expected. It is experimentally found that this condition does not result in bonding of the particle to the substrate. Note that there is no indication of any jet formation from the 400 meter per second impact, but a jet like ejection of both stainless steel and copper from the crater is shown at the higher velocities. It is proposed that this jet like flow aids in bonding similar to that created in explosive welding. In the CTH simulations, all impacts are assumed to result in bonding unless a fracture stress value is predicted.

Comparing the experimental result in Figure 2 to the 700 meter per second impact shown in Figure 9 reveals both similarities and differences. They both show a gradual decrease in the substrate height away from the impact site. They both show a lip angled away from the splat. However, Figure 2 shows that the lip is composed mostly of copper, and the numerical result shows the opposite. The penetration of the splat is overpredicted by the numerical simulation. This may be due to improper modeling of the large strain rates, or incorrect material properties. The copper may be stronger than modeled due to the small grain size associated with the rapid cooling during powder for-

mation. And the stainless steel grain size is comparable to the splat size, which will make the material properties anisotropic. In fact, the resulting crater that is formed experimentally is typically not axi-symmetric (see figure 3).

Figure 10 shows the flattening ratio and the crater depth calculated as functions of impact velocity. These agree reasonably well with the experimental measurements shown in Figure 5. The flattening ratio was determined by using the distance from the crater center to the tip of the crater lip as the splat radius. The experimental trends are reproduced: the flattening ratio is largely independent of the impact velocity, and the crater depth increases monotonically with impact velocity.

The pressure generated by the impact as a function of position and time can be obtained from the computer simulations. However, the peak pressure can be easily estimated from physical properties. The peak pressure magnitude is approximated by half the product of the particle density (9 gm/cm^3), times its impact velocity, times the speed of sound in the particle (3300 m/s). The pressure at the impact point reaches this peak in a time period that can be approximated by the particle diameter divided by the impact velocity (approximately 50 nano-seconds). It is these large pressures (on the order of 5 GPa), combined with the large deformations of the particle and substrate, that will expose clean surfaces and result in bonding. CTH assumes that all contacting surfaces result in an intimate bond between the layers. So, unfortunately, this code cannot be used to determine the critical velocity for bonding.

4. Conclusions

By both numerical and experimental methods, it has been demonstrated that cold spray deposition of copper onto stainless steel substrates results in significant cratering of the substrate. Greater impact velocity results in greater depth craters. It was also shown that the radius of the resultant splats

was insensitive to the impact velocity, except for velocities too small to be of interest in cold spray processes. Geometric sizes of the splat and crater are found to scale with the initial particle diameter. It is proposed that the large deformations caused by the jetting of both substrate and particle materials from the crater promotes bonding of the particle to the substrate. It is not required to melt either the particle or the substrate to obtain high bond strengths.

5. References:

- A. P. Alkhimov, A. N. Papyrin, V. F. Dosarev, N. I. Nesterovich and M. M. Shuspanov, U. W., "Gas Dynamic Spraying Method for Applying a Coating," Patent 5,302,414, April 12, 1994.
- E. S. Hertel, R. L. Bell, M. G. Elrick, A. V. Farnsworth, G. I. Kerley, J. M. McGlaun, S. V. Petney, S. A. Silling, L. Yarrington, Lance CTH: A Software Family for Multi-dimensional Shock Physics Analysis, Presentation at 19th International Symposium on Shock Waves, Marseille, France, July 26-30, 1993.
- B. Crossland, Explosive Welding of Metals and its Application, Clarendon Press, Oxford, 1982.
- P. J. De Groot and L. Deck, Surface Profiling by Analysis of White-light Interferograms in the Spatial Frequency Domain, J. of Modern Optics, Vol. 42, No. 2, pp. 389-401, 1995.
- R. C. Dykhuizen and M. F. Smith, "Gas Dynamic Principles of Spray," Journal of Thermal Spray Technology, Vol. 7, No. 2, pp. 205-212, 1998
- D. L. Gilmore, R. C. Dykhuizen, R. A. Neiser, T. J. Roemer and M. F. Smith, Particle Velocity and Deposition Efficiency in the Cold Spray Process, Journal of Thermal Spray Technology, submitted, 1998.
- R. C. McCune, A. N. Papyrin, J. N. Hall, W. L. Riggs, and P. H. Zajchowski, "An Exploration of the Cold Gas-Dynamic Spray Method for Several Materials Systems," pp. 1-5 of "Thermal Spray Science & Technology," Eds. C. C. Berndt and S. Sampath, ASM International, Materials Park, OH-USA, 1995, 774+ pages.
- R. A. Neiser, J. E. Brockman, T. J. Ohern, M. F. Smith, R. C. Dykhuizen, T. J. Roemer and R. E. Teets, "Wire Melting and Droplet Atomization in a High Velocity Oxy-Fuel Jet," pp. 99-104 of "Thermal Spray Science & Technology," Eds. C. C. Berndt and S. Sampath, ASM International, Materials Park, OH-USA, 1995, 774+ pages.
- H. El-Sobky, Mechanics of Explosive Welding, Chapter 6 of Explosive Welding, Forming and Compaction, Edited by T. Z. Blazynski, Applied Science Publishers, London, 1983.
- D. J. Steinberg, S. G. Cochran and M. W. Guinan, A Constitutive Model for Metals Applicable at High Strain Rate, J. Appl. Phys. Vol 51, p. 1498, 1980.
- D. J. Steinberg, C. M. Lund, A Constitutive Model for Strain Rates from 10^{-4} to 10^6 sec^{-1} , J. Appl Phys. Vol 65, p. 1528, 1989.
- A. O. Tokarev, "Structure of Aluminum Powder Coatings Prepared by Cold Gasdynamic Spraying," Metal Science and Heat Treatment, Vol 38(3-4), pp. 136-139, 1996.

F. J. Zerilli and R. W. Armstrong, Dislocation-Mechanics-Based Constitutive Relations for Material Dynamics Calculations, J. Appl. Phys., Vol. 61, pp. 1816, 1987

6. Acknowledgments: The authors would like to thank E. S. Hertel for his patient assistance in use of the CTH code, and to K. H. Eckelmeyer and A. Kilgo for metallography analysis.

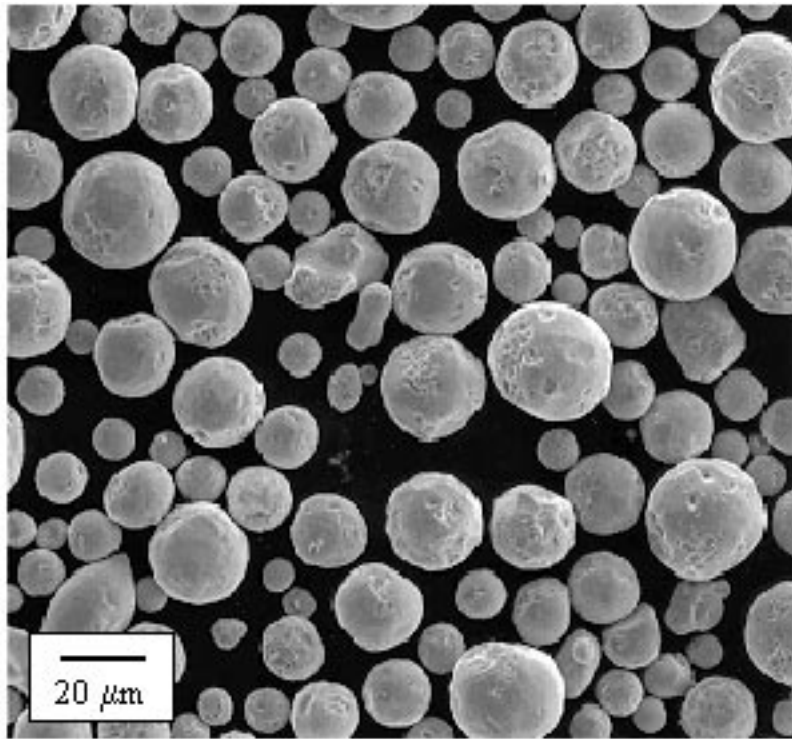


Figure 1: 22 micron copper powder used in the cold spray experiments.

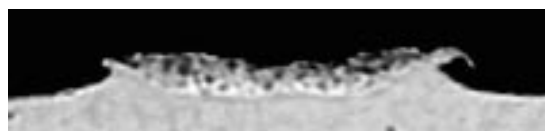


Figure 2: Cross-section of a splat created by the impact of a 700 meter per second copper particle onto a stainless steel substrate. Note the stainless steel that has been ejected from the crater which appears on the lower surface of the splat edge.

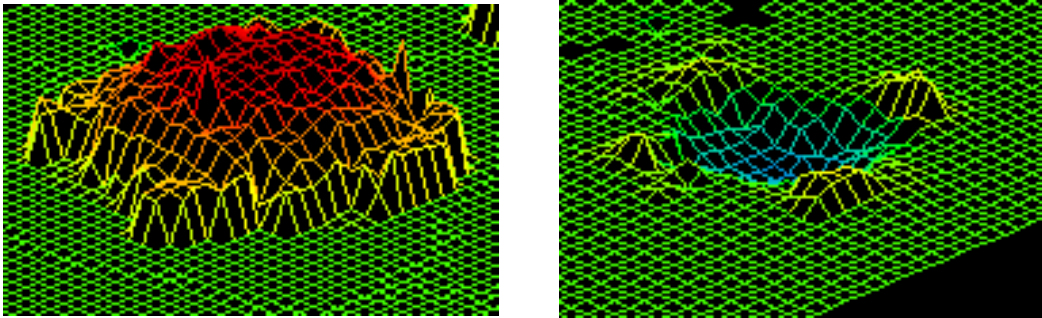


Figure 3: profilometer results for a splat and its crater from a 600 m/s impact.

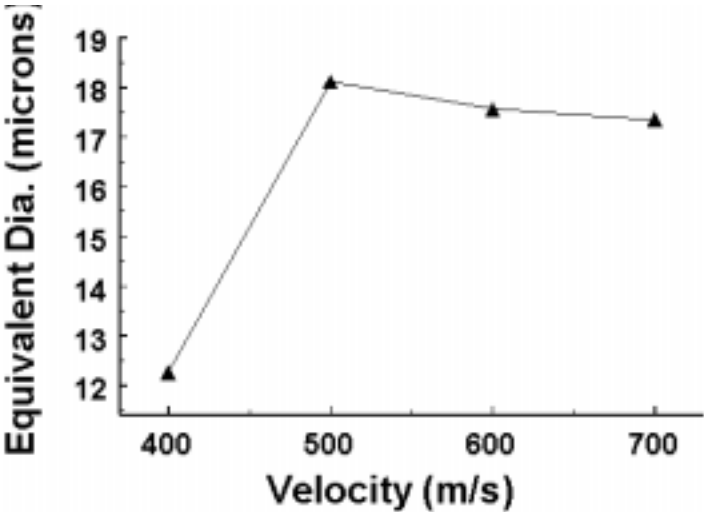


Figure 4: Experimentally measured mean particle diameter as a function of particle velocity.

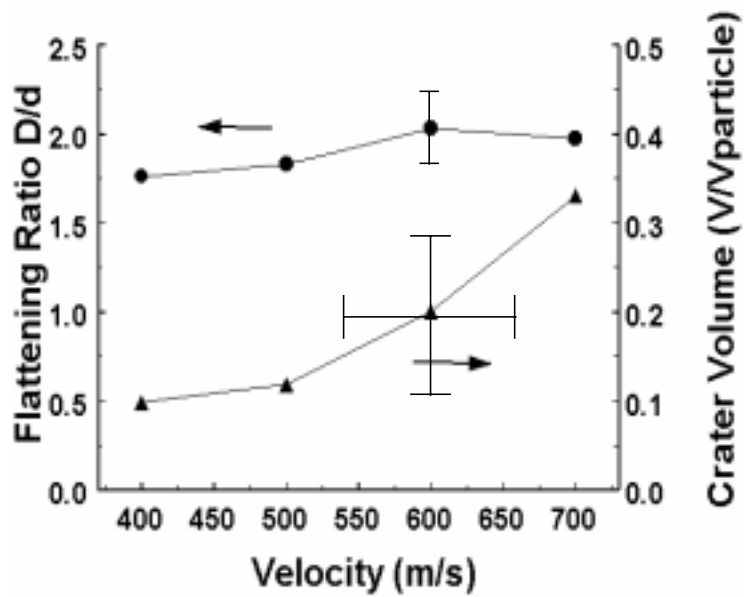


Figure 5: Experimentally measured splat ratio and crater volume as a function of impact velocity. The crater volume is non-dimensionalized by scaling with the particle volume.

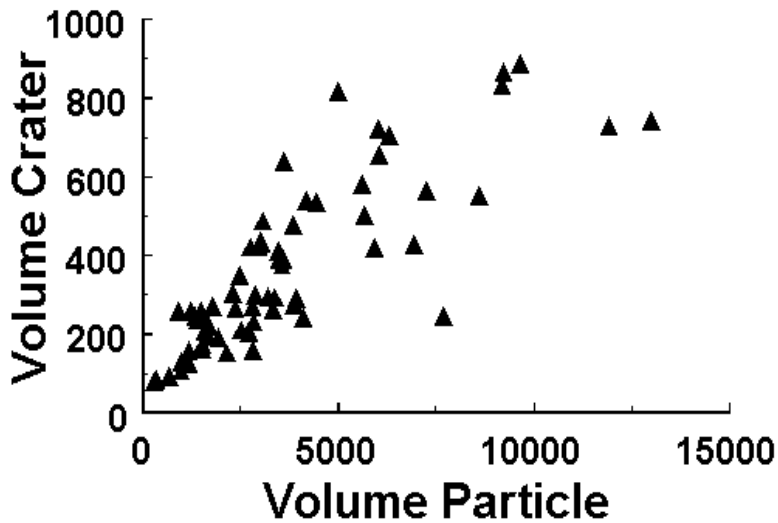


Figure 6: Volume of crater plotted against volume of particle (in cubic microns) from the 500 meter per second data set.

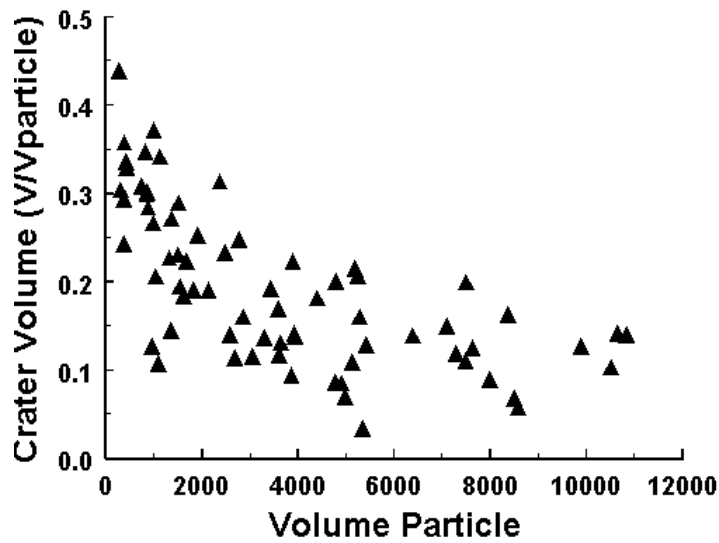


Figure 7: Non-dimensional crater volume plotted against volume of particle (in cubic microns) from the 600 meter per second data set.

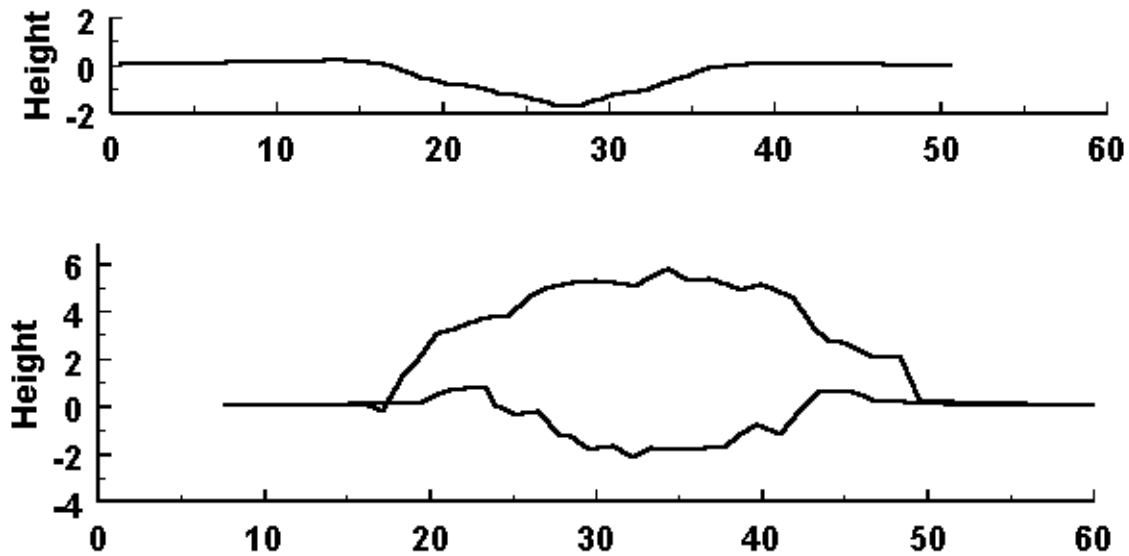


Figure 8: Comparison of crater geometry for a bonded particle (below), and a non-bonded (above) impact. Coordinates in microns.

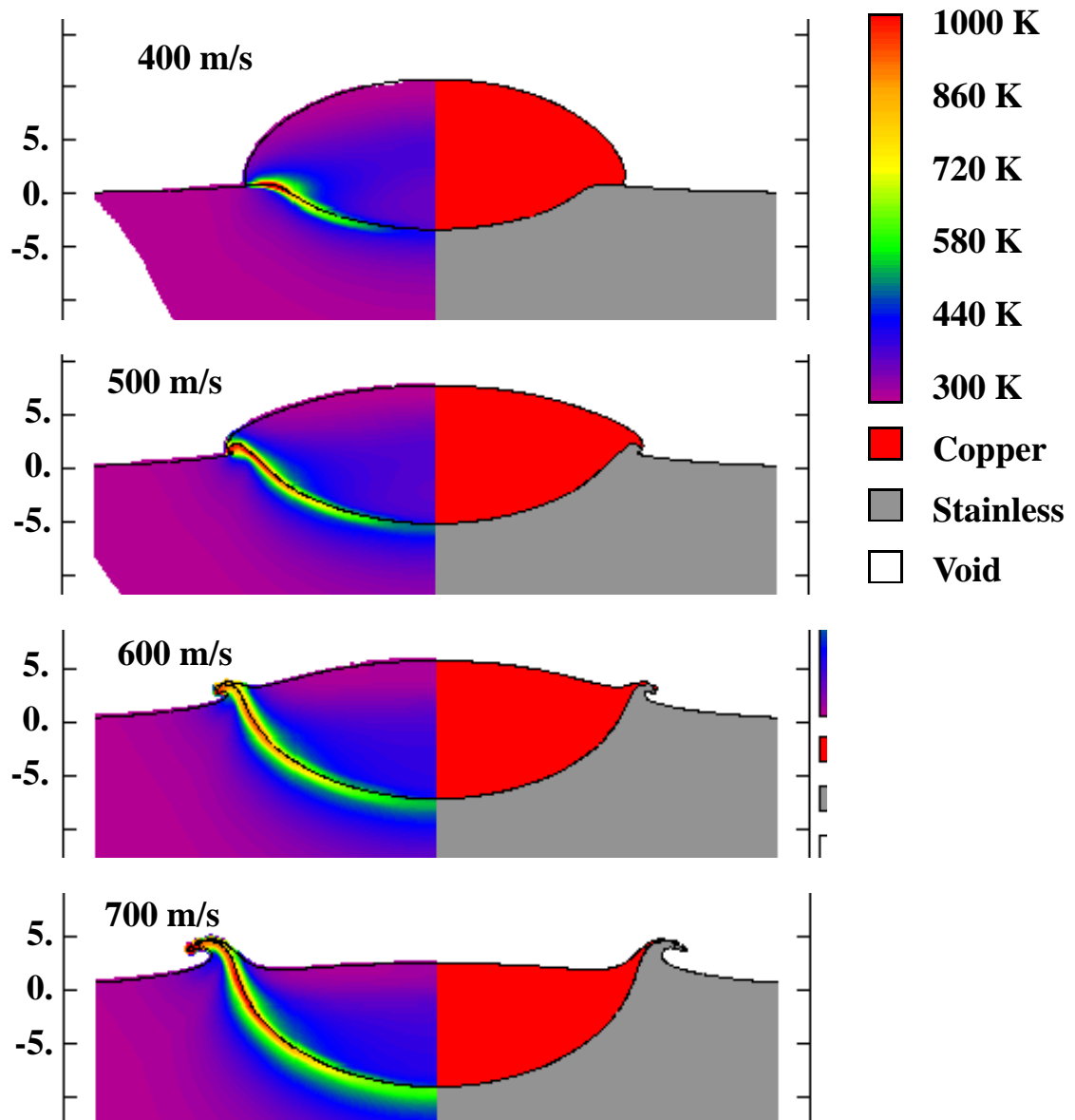


Figure 9: Splat shapes calculated by CTH. Left side shows temperature, right side shows material type. The original substrate surface is at 0 microns on the left-hand scale.

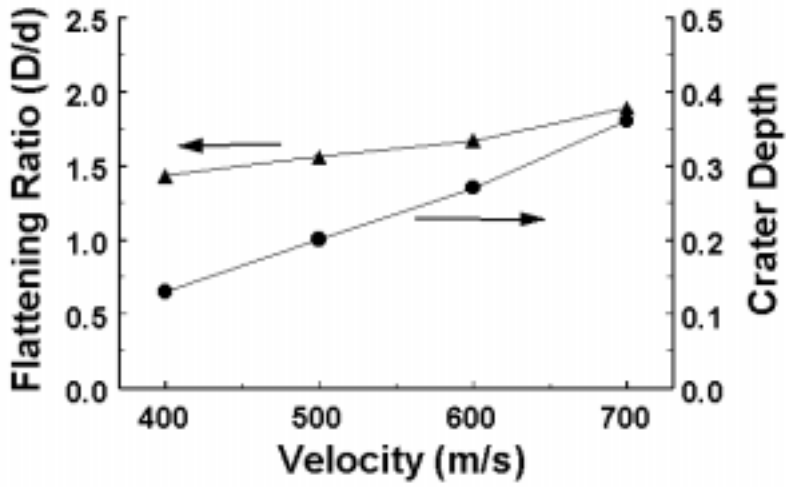


Figure 10: Calculated flattening ratio and crater depth as a function of velocity. Crater depth is non-dimensionalized by the particle diameter.